Role of Thermal Waters in The Formation of Lithium Deposits in The Salt Flats: A Critical Evaluation at Laguna Verde in The Chilean Andes

Mohammad Ayaz Alam, Adolfo Muñoz

Departamento de Geología, Universidad de Atacama, Avenida Copayapu 485, Copiapó, Región de Atacama, Chile

Keywords

Geothermal, geochemistry, lithium, salt flat, salar, Andes, Laguna Verde, Atacama, Chile

ABSTRACT

Despite lithium (Li) rich brines in salt flats often being associated with geothermal systems, most salt flats do not have an active present-day geothermal system to evaluate this association, making this association somewhat speculative. However, a salt flat in the Chilean Andes with a hypersaline lake – Laguna Verde (LV) – within a closed basin encircled by a series of volcanoes, an active geothermal system with surface manifestations, and outcrops of the potential Li source rocks, provides an excellent opportunity for this evaluation. The study area has outcrops of mostly andesitic-dacitic rocks with the limited occurrence of rhyolitic rocks (sequences with ignimbrites and glass-rich ash), reported in the boreholes drilled in the area for mineral exploration. From these lithologies (primary sources), Li is released through leaching by geothermal fluids, active intermittently from the Miocene to the present day. The LV geothermal system consists of an outflow zone on the lake's southern margin, where more than 20 hot springs with temperatures up to 47°C are located. This system's upflow area is 25 km SSW of LV, represented by fumaroles located in the Nevado Ojos del Salado volcano's central crater. The considerable distance between upflow and outflow zones (i.e., the geothermal system's extension) is likely to cause requilibration(s) during the long-distance travel of thermal water, leading to underestimation of reservoir temperature (85 and 90°C with Na-K-Mg and silica geothermometers, respectively). Whereas Li concentration in the hot springs is 2.76 to 4.46 mg/L, in Peñas Blancas River that feeds LV after passing through the volcanic environment (rocks rich in Li), thus getting enriched in Li, it is 0.59 to 0.76 mg/L. Li contribution over six times the non-thermal water envisages the importance of the thermal waters in Li release and transport from the source rock to its eventual concentration in LV.

1. Introduction

The role of geothermal fluids in the formation of lithium (Li) deposits is often speculative, as an active geothermal system is not always there to associate it with. However, all brine deposits with economic Li concentrations are associated with fossil geothermal systems (Hickson and Coolbaugh, 2017). Furthermore, geothermal activity is not an exclusive requirement for forming Li-rich brines in the salt flats, as non-thermal devitrification processes and weathering processes can release Li from volcanic rocks (Price et al., 2000).

1.1 Background and context

Salt flats (known as 'salars' in Chile and other Latin American countries) are evaporitic sedimentary deposits formed in endorheic (closed) basins. Their formation requires evaporation rates higher than those of precipitation, which facilitates the concentration of residual salts until forming a saline crust on the surface. However, not all salt flats have economic concentrations of Li. Thus, there are two ways of Li enrichment in the salt flats, which could be concurrent, as in the case of the SLV.

1.1.1 Li enrichment through geothermal fluids

Bradley et al. (2013) reviewed commercially viable Li deposits in the salt flats, and based on their distinctive aspects, proposed a model for Li enrichment of brines from geothermal sources. Accordingly, these deposits have several common first-order characteristics; viz. arid climate, endorheic basin containing a salt flat, tectonically driven subsidence, igneous rocks or associated geothermal activity, Li source rocks, one or more aquifers, and sufficient time for Li concentration.

More recently, Hickson and Coolbaugh (2017), through a similar analysis, proposed necessary factors for Li rise enrichment of brine, similar to those proposed by Bradley et al., (2013). These factors include (i) a Li source (rocks), (ii) an extraction mechanism (geothermal or meteoric), (iii) a transport mechanism (flow of Li-rich fluids), (iv) an endorheic (closed) basin, (v) sufficient solar evaporation rate, and (vi) mass Li flux and limited competition from dissolved salts, which takes into account the scale of the process. Moreover, Hickson and Coolbaugh (2017) reported the factors (ii), (iii), and (vi) to be significantly influenced by the presence of the geothermal fluids.

The Li-enriched brine formation process starts from the source rocks in an endorheic basin. . The tectonic subsidence rate of the closed basin controls the relationship between sediments and salts that fill the basin. The subsidence-dominated basins contain more clastics and thus maintain permeability at depth, allowing fluid escape. On the other hand, the basins with more salts tend to lose permeability at depth due to the plastic behavior of halite. Fluid leakage/descension to deeper permeable formation affects Li concentration in the dense brine that tends to infiltrate until prevented by an aquitard or impermeable basement rocks.

Lithium extraction from source rocks can be triggered by geothermal fluids and/or meteoric fluids (The role of the latter is discussed in the following subsection 1.1.2). Geothermal fluids can make the extraction and transport process more efficient by selectively dissolving Li relative to other elements in volcanic rocks and glasses (Bradley, 2013; Hickson and Coolbaugh, 2017). This is demonstrated by empirical data on the composition of thermal fluids as a function of

temperature. For example, Li/Mg (Fouillac and Michard, 1981) and Li/Na (Kharaka and Mariner, 1989) ratios systematically increase by multiple orders of magnitude with increasing temperature. In addition, pH controls the dissolution capacity of silicates, and geothermal fluids, especially in the outflow zone, can have very acidic levels (pH<2), thus dissolving the Li-bearing silicates more readily. For example, Houston (2011) noted that brines in the Central Andes have high Li/Mg ratios, which are difficult to explain under surface weathering conditions, especially in volcanic terrains, where groundwater commonly has high Mg concentrations but is easier to explain by invoking geothermal fluids. Likewise, there is an excellent spatial relationship between felsic volcanism, geothermal activity, and Li brines or Li-enriched clays; e.g., Clayton Valley in the USA (Davis et al., 1986), Atacama salt flat in Chile (Lowenstein and Risacher, 2009), Qaidam Basin in China (Yu et al., 2013). For example, in Qaidam Basin, Li enrichment of the alluvial deposits since the last glacial period is attributed to Li from thermal springs located 300 km upstream (Yu et al., 2013).

The transport occurs in solution through the flow that deposits the fluids in the basin and can be meteoric and/or thermal (Bradley, 2013). The evaporative concentration of surface water within closed basins over time leads to the residual concentration of dissolved salts rich in sodium, potassium, chlorine, carbonate species, boron, and Li (Hickson and Coolbaugh, 2017).

Finally, the most critical factor determining whether a basin can be enriched in Li is whether the basin remains closed or not (Hickson and Coolbaugh, 2017). Although saline/hypersaline lake basins owe their genesis to corresponding tectonic mechanisms, they are maintained for long periods only when evaporation exceeds precipitation. However, if the lake basin is breached eventually along the watershed due to tectonic uplift, such lakes will consequently drain, carrying with it dissolved Li (Bradley, 2013). That explains why Li deposits in brines worldwide are located above the tropics, between 19 and 37° north or south. Of all the deposits, three are located in a semi-arid, 11 in an arid, and one in a hyperarid climate (Kesler et al., 2012).

1.1.2 Li enrichment without geothermal fluids

Li-enrichment of brines in salt flats and without geothermal fluids is similar to that with geothermal fluids, except that the transport medium is meteoric water. Thus the process is slow and takes place at relatively lower (i.e., ambient) temperatures. Price et al. (2000) showed evidence of non-thermal devitrification and weathering processes that can release Li from the glassy part of the volcanic rocks in Clayton Valley, Nevada. Weathering and diagenesis may act as an extraction mechanism through the alteration of Li-bearing minerals. Thus geothermal or hydrothermal activity is not an indispensable requirement for the formation of Li rich brines.

Unlike geothermal fluids, Li's enrichment of meteoric water is slower, resulting in lower brines (Hickson and Coolbaugh, 2017). However, the mechanism is the same; i.e., Li is leached from the source rocks, accumulates in endorheic basins, and enriches by evaporation to form deposits with residual concentrations.

1.2 Study area

The Salar de Laguna Verde (SLV; *salar*: salt flat or salt pan is referred as 'salar' in Chile and other Latin American countries) has high concentration of Li, potentially driven by an active geothermal system with surface manifestations, and from distal sources through rivers flowing

into the Laguna Verde (LV) hypersaline lake. This provides an opportunity to evaluate the contribution of Li from different potential sources. Furthermore, understanding Li's release process from the source rocks and its subsequent accumulation in the SLV could form part of an exploration guide applicable to similar Li deposits worldwide. The study area is part of the Central Andean dry Puna ecoregion that occupies the southwestern portion of the Altiplano (Andean high plateau) and is located east of the Atacama Desert. The area is characterized by a cold desert climate, marked by hyperaridity, as testified by the presence of a partially mummified cow close to Laguna Verde (Figure 1).

Figure 1: Thermal pool at Laguna Verde with a partially mummified cow in the inset.

Figure 2: Location of the study area.

Laguna Verde (LV, 26°53′S 68°28′W, Figure 2), a hypersaline lake within a salt flat of the same name – Salar de Laguna Verde, is named so (Laguna Verde = Green Lagoon) for its (turquoise) green color because of high salinity. The lake has a surface area of about 15 km^2 within a hydrographic basin (Code 3030, DGA; acronym in Spanish for the Directorate General of Water) of approximately 1075 km^2 in the administrative Region of Atacama (Chile). It is located in the Andean Cordillera at an elevation of 4,328 m above mean sea level, 265 km east-northeast of the regional capital Copiapó, on the highway (*Ruta CH-319*) to the San Francisco mountain pass (23 km east of LV) at the Argentine border.

1.3 Scope of the present study

The removal and transport of Li from source rocks is favored by geothermal fluids compared to meteoric (non-thermal) devitrification processes, as in the former case, Li is dissolved more readily into higher temperature waters. Furthermore, the increase in volcanic activity since the Late Pliocene and the hyper-arid climatic conditions prevailing since the Late Miocene have provided the requirements and time needed to raise Li concentrations to an economically profitable level. In this context, the present study aims to assess the role of geothermal fluids in the removal, transport, and concentration of Li in SLV. It involves (i) geological characterization of the study area to identify and map the geological formations that potentially contribute Li and the thermal manifestations, (ii) determining the chemical and isotopic composition of the water (thermal as well as non-thermal, viz. lake, river water) samples, and (iii) identification of the geochemical processes responsible for Li concentration in the SLV.

1.4 Material and methods

Mapping of the local geology and surface geothermal manifestations was done through field visits to the SLV, interpreting high-resolution satellite imagery and available geological maps of the sector prepared by the National Geology and Mining Service (SENGEOMIN), Chile.

In situ measurements of physicochemical parameters of thermal and non-thermal waters from the study area were carried out during the aforementioned field visits, and samples were collected for subsequent analysis; namely for (i) major and trace elements, using Inductively coupled plasma mass spectrometry (ICP-MS; US EPA Method 200.8; Activation Geological Services, Coquimbo, Chile), ionic chromatography (IC; EPA Method 300.1; Activation Geological Services, Coquimbo, Chile), alkalinity (carbonate-bicarbonate) analysis by titration (SM 2320 Method of NEMI, USGS Activation Geological Services, Coquimbo, Chile), and (ii) isotopic analysis of δ^2H (or δD) and $\delta^{18}O$ using Accelerator Mass Spectrometry (AMS; ISO/IEC 17025; Beta Analytic Radiocarbon Laboratory, Miami, Florida). Binary diagrams of major elements, together with Piper, Spider, Schoeller, and Stiff diagrams, were used to present and interpret chemical data on water. Solute geothermometers were used apart from variation diagrams for thermal waters.

2. Geology of the study area

The objective of the characterization of geological units is to determine possible Li sources. The geological profiles based on borehole data up to 250 m depth carried out by SRK (2011) show a heterogeneous filling of the basin. It can be highlighted that the andesitic and dacitic rocks are the most abundant, and therefore, the primary Li sources; as, according to Zampirro (2004),

felsic rocks are richer in Li. Besides, ignimbrites and pumices (both relatively richer in glasses) may have released significant amounts of Li.

The study area is located in the western part of the southern end of the Central Volcanic Zone (CVC; Stern, 2004), which is the northern segment of the Chilean volcanic arc. It is separated from the Southern Volcanic Zone (SVC; Stern, 2004) by the Pampean Flat Slab (PFS; Stern, 2004), devoid of volcanic activity. The CVZ is a segment of the Andean Volcanic Belt, comprising active volcanoes of Argentina, Bolivia, Chile, and Peru. The CVZ is one of the largest volcanic provinces in the world (González et al., 2009). It contains 44 active volcanic edifices and 18 minor active centers located above 4,000 m a.m.s.l., and at least six potentially active caldera systems. The crustal thickness is 70 km and is located 120 km above the subducted plate. Nevado Ojos del Salado (located in the study area), Lastarria, San Pedro and Parinacota volcanoes are well-known volcanoes within the CVZ. The basement of the CVZ comprises sedimentary, volcanic, and intrusive rocks of the Upper Paleozoic (Clavero et al., 2012), on which the volcanic structures of andesitic stratovolcanoes and complexes of dacitic domes emerge. Pyroclastic flows, tephra fall, avalanches of debris, and flow deposits of blocks and ashes, among others, are associated with these volcanic centers (Stern, 2004).

Of the rocks of the CVZ, the oldest ones are of Upper Miocene age that correspond to stratovolcanoes of andesitic and dacitic compositions (Barrancas Blancas, Mulas Muertas, and Laguna Verde volcanoes; Msv), emerging from the edges of the Wheelright Caldera (Baker et al., 1987; Clavero et al., 2012). They are followed in age by the volcanic rocks of the Lower Pliocene, represented in the study area by Peñas Blancas and El Ermitaño volcanoes (Piv a), both of andesitic to dacitic compositions, with some basaltic lavas. These rocks also outcrop through annular fractures of the Wheelright Caldera. They are similar in age to small outcrops of an adventitious cone of basaltic composition south of the Peñas Blancas volcano (Piv c) and a dacitic dome of the Mulas Muertas volcano (Piv e). Subsequently, the Laguna Verde Ignimbrite was deposited, which corresponds to an extensive rhyolitic pyroclastic flow divided into four flow units that fill Laguna Wheelright and Laguna Escondida depressions. In the Upper Pliocene, lobed lava flows (Psv) of andesitic to dacitic composition were deposited in the southern part of the study area and are randomly distributed (e.g., Mesetas Negras volcano). The San Francisco Ingnimbrites (Plisf) of rhyo-dacitic composition (Clavero et al., 1997) was deposited during the Lower Pleistocene. Its distribution is restricted to small outcrops at the edges of the San Francisco ravine at the southeastern edge of the study area. During the Pleistocene-Holocene, different volcanic complexes located mainly along the border with Argentina emerged (e.g., Nevado Ojos del Salado, El Muerto, Incahuasi, San Francisco, and Falso Azufre volcanic complexes). The rocks of this age are represented by lavas of dacitic composition (PlHv a), dacitic domes (PIH b), pyroclastic deposits with blocks and ashes (PlHv c), pyroclastic deposits PlHv d), laharic flows PlHv h, El Fraile Ignimbrites PlHvf, and pumice deposits PlHv j. On the other hand, within the study area, large areas affected by hydrothermal alteration have been recognized, mainly linked to dome complexes, caldera structures, and Pliocene-quaternary volcanoes' hydrothermal activity.

2.1 Tectonics and Structure

The tectonic evolution of the study area can be understood through the Andean Cycle that led to the current configuration of the different morphostructural units of the Andean Cordillera

(Charrier et al., 2007). The Andean Cycle represents the successive stages of construction of the Andes beginning in the Early Jurassic period, in which subduction of the Mariana type at the western bank of South America and the current Coastal Cordillera de la Costa is formed with a back-arc basin of the extensional regime. The stages after the Late Cretaceous are characterized by tectonic shortening (erosion) due to faster subduction of the slab that led to a transpressive regime in the continental part (Amilibia et al., 2008). These significant periods of deformation, known as tectonic phases, produced significant paleogeographic changes, including tectonic inversion and lifting of the basins formed during the previous extensional regime, which gave rise to the Domeyko mountain range (Cordillera de Domeyko) and the creation of foreland basins. The pre-Andean depression resulted from the deformation and uplift of the western cordillera and the displacement of the magmatic arcs to the east, limited to the west by the Domeyko Range and towards the east by the Claudio Gay mountain range (Cordillera de Claudio Gay). The latter uplifted during the Inca phase, with an inversion of basins that lead to the closure and formation of endorheic basins in what is now known as the Atacama Altiplano or Puna de Atacama.

In the Laguna Verde Basin, located with the Atacama Altiplano or Puna de Atacama, the eastern domain includes the Upper Miocene to Quaternary volcanic edifices of the active volcanic zone of the central Andes, which occupy a depression related to the Claudio Gay mountain range, which limits them to the west (Clavero et al., 2012). Although volcanic complexes have suffered varying degrees of erosion, they remain structurally intact for the most part, with no evidence of having been affected by significant deformation episodes. The presence of alignments of craters and volcanic buildings with preferential directions NW-SE, NE-SW, and E-W indicates that blind faults and/or fractures with the same orientations, located in the pre-volcanic basement, could have served as conduits for the ascent of quaternary magmas to the surface (Clavero et al., 2012). Someofsuch faults and second-order fractures manifest on the surface as small fault escarpments or lineaments that sometimes dissect lava units, domes, or emission centers.

2.2 Hydrology

The Laguna Verde hydrogeological basin has an area of approximately 1,000 km^2. It is an endorheic basin with few streams that flow mainly in the summer. The hydrogeological delimitation is quite difficult because of limited information on the subsurface geology, mostly from the hydrogeological map of the Campo Piedras Poméz-Laguna Verde Basin (Santibáñez et al., 2006) and Environmental Impact Study of the Cerro Casales Mining Project (MWH, 2011). Nevertheless, it is believed that part of the underground flow migrates to the Campo de Piedras Pómez (west of the SLV) to the east, in turn to the basin of the Lamas River (Santibáñez, 2006). The basin fills consist of an alternation of volcanic material, consisting of pyroclastic rocks and andesitic-dacitic lavas and, to a lesser extent, sediments of volcanic origin with little transport, consisting mainly of gravels and coarse sands with little fine material. The main water stream of the basin is the Peñas Blancas River that crosses the homonymous plain and makes the greatest contribution to the Laguna Verde. This hypersaline lake is also fed by other streams originating from cold springs, important ones being the Agua Dulce stream and the ravine of the Falso Azufre volcano.

The principal aquifers and the cold springs from which the streams originate are hosted in the Barrancas Blanca and Peñas Blancas highlands. These generally unconfined (phreatic) aquifers

(PIQa and PliPla) have transmissivity between 3,000 and 4,000 m^2/day (EDRA, 1999) and a storage coefficient of about 0.005, i.e., high to moderate. The deposits of medium to low hydrogeological importance correspond to local intergranular aquifers with irregular productivity. They include Pliocene and Quaternary volcanoclastic deposits (PliQvc), Pliocene and Quaternary pyroclastics (PliQp), Quaternary ignimbrites (Qi), Quaternary colluvial and mass-transport deposits (Qc), and Quaternary saline deposits (Qs). They generally form unconfined (phreatic) and sometimes semiconfined aquifers with an average transmissivity of 1,000 m^2/day and a storage coefficient of 10×10^{-5} (EDRA, 1999). The formation with low hydrological potential corresponds to the Eocene-Miocene lavas (EMv), Pliocene, and Quaternary lavas (PliQv) and the Quaternary lake deposits (Ql) with a transmissivity of 50 and 100 m^2/day and storage coefficient of 9×10^{-4}. Similarly, but in fissured rocks, aquifers consisting of Eocene-Miocene sedimentary rocks (EMs) are found. Laguna Verde Ignimbrite (Pilv) is distributed mainly around the Laguna Verde in the eastern part of the basin within the fissured aquifers of moderate to high hydrological importance. Lastly, the aquicludes correspond to Tertiary and Quaternary domes and Miocene lavas (PzQ), with zero capacity to store and transmit water, constituting the impermeable basement.

2.2 Hydrochemistry

Of the two hydrochemical studies carried out previously in the study area, the first one is a part of the geochemical characterization of the surface water bodies of the administrative regions I, II, and III. It provides an approximation of the chemical composition of water in terms of major ions (Risacher et al., 1999).

Table 1. Qualitative comparison of evaporated water with Laguna Verde brine (Risacher et al., 1999).

Sample	Source	pH	HCO_3	Cl	SO_4	B	Si	Na	K	Li	Ca	Mg	S.D
LAV-1	LV	7.56	5.89	92,500	13,800	513	13.3	57,700	5,400	204	533	2,380	
8+2+3	Mixture	7.89	5.57	90,800	14,700	494	13.7	56,400	7,660	318	441	1,960	0.04
LAV-8	PBR	7.79	6.11	83,400	21,600	674	16.2	58,400	6,400	229	674	532	0.2
LAV-3	DSP	7.63	6.01	100,000	6,500	594	14.1	50,200	7,260	453	2,210	5,140	0.33
LAV-6	LVH	7.98	29.9	84,800	20,200	358	18.3	61,000	6,360	186	9,23	32.3	0.8
LAV-7	PBT	9.77	250	75,500	21,200	562	31.5	60,000	7,200	185	0,53	1.8	0.9
LAV-2	ADR	10.1	1,220	41,200	23,300	396	54.7	62,100	5,950	155	0,37	1.33	1.05

Note: The mixture (8+2+3) corresponds to 50% (8) + 40% (2) + 10% (3). LV: Laguna Verde, PBR; Peñas Blancas River, DSP: Diffuse spring, LVH: Laguna Verde Hot Spring, PBT: Peñas Blancas Tributary, ADR: Agua Dulce River

In the present study, a hydrochemical balance comparing the composition of the Laguna Verde water with that of the inflowing streams has been attempted. It was determined, with a standard deviation (S.D.) of about 0.04, that Laguna Verde is fed 50% by the Peñas Blancas River, 40% by the Agua Dulce River and 10% by the Falso Azufre Ravine (Table 1). The second hydrochemical study is part of a technical report of the Salar Laguna Verde Project and other properties held by the South American Lithium Company (Hiner, 2009). Based on ICP-MS analysis, it reports Li concentration of 211 to 232 mg/L for Laguna Verde and 2.87 mg/L for thermal water samples collected from the SLV in September 2009.

2.3 Geothermal manifestations

Within the Laguna Verde basin, thermal pools (formed by incipient hot springs) are located near Laguna Verde. At the same time, fumaroles in the Ojos del Salado volcano crater were identified by the images of steam emission taken by an expedition team of the extreme tourism company "Extrem Events" in December 2019. The fumarolic activity has been previously reported in the “Japanese Route” sector of the Nevado Ojos del Salado in 1937 and 1956. More recently in November 1994, an intermittent gray column of water vapor was observed by the mountaineers in the morning hours near the Amistad Refuge, located 6,100 meters above sea level (Camus, 2001).

Thermal springs with a profuse or diffusive flow are found throughout the southwestern edge of Laguna Verde, which discharge below the level of the Laguna Verde Ignimbrite (Pilv) outcrops. These discharges are surrounded by argillic alteration, silica sinter and generally serve as habitat for thermophilic organisms and sometimes present chlorite and epidote mineralization. The maximum measured discharge temperature was 47°C in November 2017, prior to the summer season, while a temperature of 41°C was recorded in April 2018 after melting of the Altiplanic Winter snow at the same place (Table 2). Similarly, discharge temperature of the thermal manifestations located on the southwestern edge of Laguna Verde measured in March 2019 was maximum (42°C) at the same point (Table 2) with a decreasing temperature towards northwest up to 12.2°C.

Table 2: Temperature, type, and location reference of the water samples

Sample point	Location reference	Sample type	T° (°C)	Date
M1	Falso Azufre volcano ravine	Spring	20.6	15-04-2018
			17.2	06-03-2019
M2	Laguna Alta	Lake	5.7	06-03-2019
M3	Agua Dulce River	Stream	15.6	15-04-2018
			6.7	06-03-2019
M4	Thermal pool	Hot spring	47.0	21-11-2017
			45.0	21-11-2017
			41.2	15-04-2018
			42.1	06-03-2019
M5	Laguna Verde	Lake	5.0	21-11-2017
			10.3	15-04-2018
M6	Peñas Blancas River (northern tributary)	River	19.9	06-03-2019
M7	Peñas Blancas River (main stream)	River	17	15-04-2018
			18.6	06-03-2019
M8	Lamas River	Spring	14.4	15-04-2018

In the Lamas River, outside the study area in the Piedras Pómez basin (48 km southwest of Laguna Verde), a temperature of 14.4°C was recorded with the ambient temperature of -15°C.

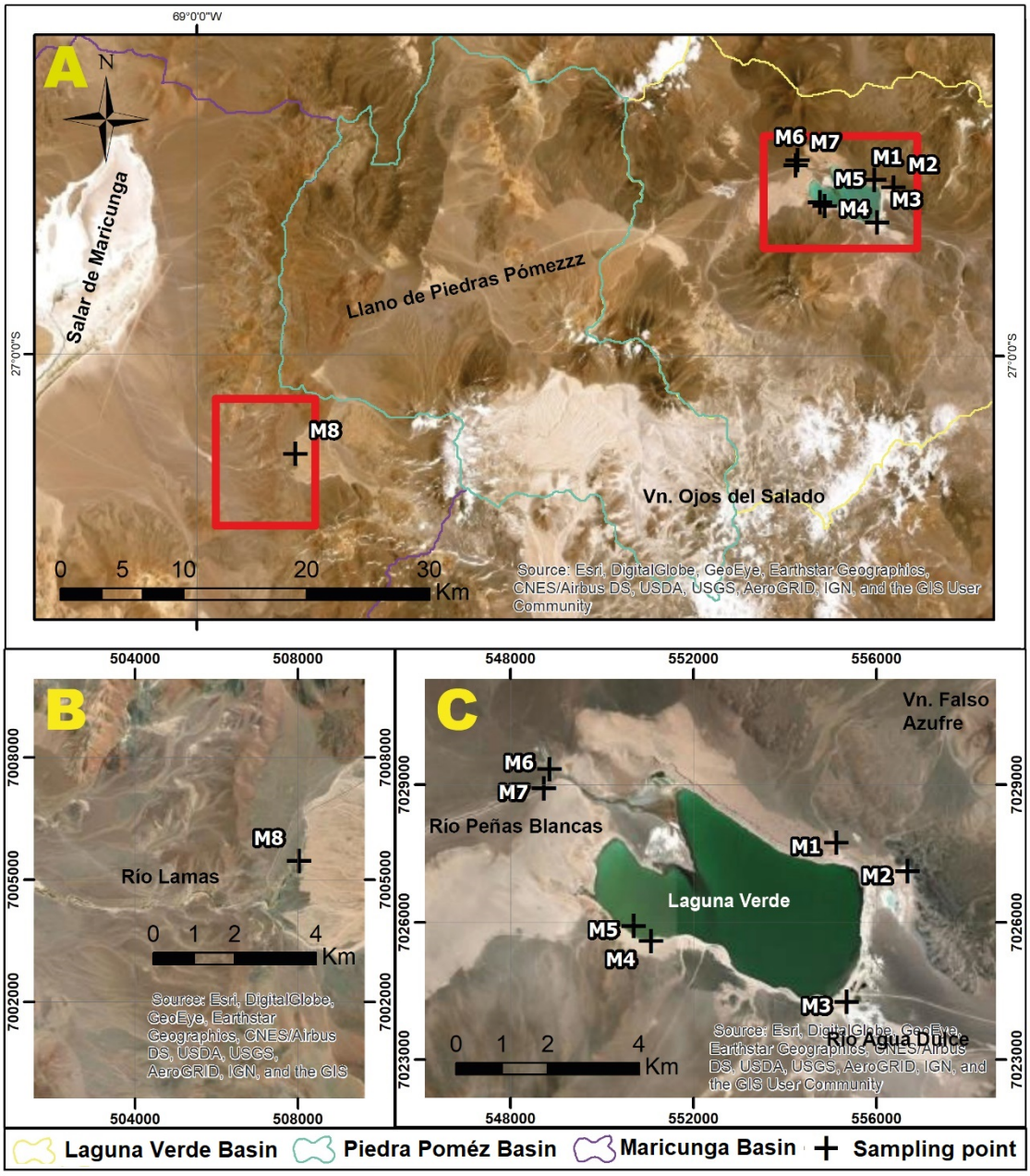

Figure 3: Water sampling points (A) with Lamas River (B) and Laguna Verde (C) sectors magnified.

3. Water chemistry and isotopic composition

A total of 15 water samples were collected at seven sampling points during field visits between 2017-2019 to determine the chemical composition and contribution of the thermal fluids and

inflowing streams to Laguna Verde (Figure 3, Table 2). An eighth sampling point was added in 2018, where a temperature anomaly was detected at a discharge in the Lamas River (Figure 3, Table 2). Also, four water samples were collected for isotopic analysis ($\delta^{18}O$ and $\delta^{2}H$) in June 2018. Additional isotopic samples were facilitated by an unrelated project (16IFI-65907) of the Universidad de Atacama. See the Table 2 for the temperature, type and location reference of the water samples.

The results of chemical and isotopic analysis are presented in Table 3 and 4 respectively.

Table 3: Results of chemical analyses (MX-YY: Sample location-Year; a,b: two nearby samples)

Parameter \ Sample	M1-18	M1-19	M2-19	M3-18	M3-19	M4-17a	M4-17b	M4-18	M4-19	M5-17	M5-19	M6-19	M7-18	M7-19	M8-18
T° (°C)	20.6	17.2	5.7	15.6	6.7	47.0	45.0	41.2	42.1	5.0	10.3	19.9	17.0	18.6	14.4
pH terreno	9.19	8.46	5.30	8.85	5.79	7.5	7.5	7.29	6.30	8.10	6.09	9.19	8.54	6.45	7.6
CE terreno (mS)	1.8	1.7	6.5	2.1	2.4	5.6	5.7	5.4	5.5	172	155	1.5	3.1	2.9	0.99
Cl (mg/L)	400	405	1.920	253	306	1,557	1,518	1,307	1,229	55,184	51,581	485	687	729	103
SO_4 (mg/L)	175	221	507	325	394	596	551	594	795	551	15,542	295	285	400	108
HCO_3 (mg/L)	71	94	237	359	441	215	210	191	220	112	115	111	84	87	210
F (mg/L)	0.65	0.55	0.10	0.79	0.10	1.2	1.1	1.1	0.10	1.1	0.10	0.10	0.49	0.10	0.65
Si (mg/L)	39	41	55	45	33	38	41	70	77	30	24	44	34	39	20
Na (mg/L)	284	292	925	416	497	1.312	1,277	1,076	1,076	12,553	12,040	459	537	547	164
K (mg/L)	30	28	125	34	35	111	105	96	88	2,724	3,895	29	57	52	21
Ca (mg/L)	23	36	243	12	19	36	35	36	43	603	935	19	28	39	8,6
Mg (mg/L)	17	15	102	4.1	7.3	16	14	18	20	1.074	1.693	7.7	6.0	5.1	9.9
Li (mg/L)	0.59	0.69	7.33	0.76	0.92	4.49	4.46	2.80	3.08	117	103	1.01	0.89	2.08	0.21
Cs (mg/L)	0.015	0.012	0.110	0.004	0.007	0.073	0.069	0.057	0.060	2.2	5.7	0.031	0.110	0.120	0.230
B (mg/L)	2.1	2.6	8.8	1,7	1.6	17	16	9.9	9,0	246	96	3.9	4.1	7.3	0.93
Rb (mg/L)	0.07	0.07	0.53	0.06	0.06	0.27	0.26	0.23	0.26	7.4	21	0.07	0.12	0.15	0.09

Table 4: Results of isotopic analyses

Sample code	Elevation (m)	$\delta^{18}O \pm 1$ (‰)	$\delta^{2}H \pm 1$ (‰)
M1-18	4,338	-8.78	-71.64
M3-18	4,335	-9.41	-68.87
M7-18	4,333	-9.28	-76.36
M8-18	4,311	-10.11	-81.42
M8-05*	4,311	-12.93	-91.8
M8-06*	4,311	-10.12	-80.9
M8-07*	4,311	-10.08	-77.33
M7-05*	4,333	-9.94	-78.69
M7-06*	4,333	-10.57	-83.01
M7-07*	4,333	-10.46	-80.73

* Samples provided by Project 16IFI-65907 of the Universidad de Atacama

4. Discussion

4.1 Chemistry and isotopic composition

The water samples were classified using Piper diagram (Figure 4). All samples are predominantly Na-Cl type, except for the M2 sample which is Ca-Mg-SO_4 type. This could be because M2 (Laguna Alta, a hypersaline pond) has a waterproof hyaline bottom that hydraulically insulates chloride-rich hot spring recharges. While, Na and Cl are the dominant ions in the samples M1, M3 to M7, these waters have significant concentrations of sulfate, being sodium chloride sulfate waters. At the same time, M8 is a mixture between sodium chloride and bicarbonate sodium waters. The enrichment in chloride may be because evaporation exceeds over precipitation in the study area, and the chlorides are also incorporated from geothermal fluids.

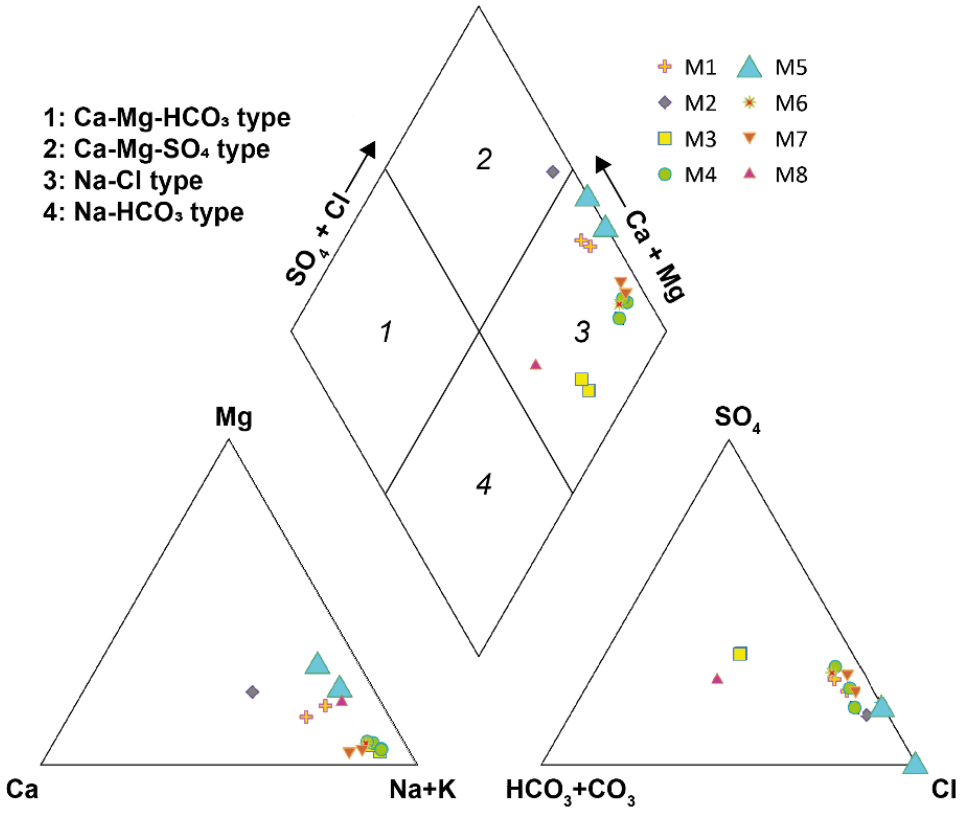

Figure 4: Piper Diagram (1952) for the SLV waters (Sample description in Table 2 and Figure 3)

4.1.1 Lithium concentration and temperature

In Figure 5, the Li contents of water versus temperature are shown, where a linear correlation can be observed, with a mean square error of about 0.90. Although the M4 samples were taken from the same location, the Li concentration decreases significantly after summer, probably due to dilution by melting snow. The M7-19 sample was collected closer to the thermal discharge zone

and contains 2.08 mg/L Li compared to M6-19 with 1.01 mg/L Li, both belonging to the Peñas Blancas River. This indicates likely mixing between thermal and meteoric waters at the southern bank of the Peñas Blancas River. In the M1 site samples collected in 2018 and 2019, both taken at the end of the summer, an increase in Li content and a decrease in temperature are observed, although the changes are subtle. This is contrary to the trend of M4 hot springs (blue line Figure 5), so it can be assumed that the origin of these waters is not geothermal. However, the above can be explained in terms of Li the incorporation as a product of non-thermal devitrification processes (Zampirro, 2004) involving snowmelt water. Between M7-18 (12 April 2018) and M7-19 (06 March 2019), there is an increase in Li concentration from 0.89 to 2.08 mg/L, respectively, a variation that could be explained by the heavy rainfalls of 2017 and 2018.

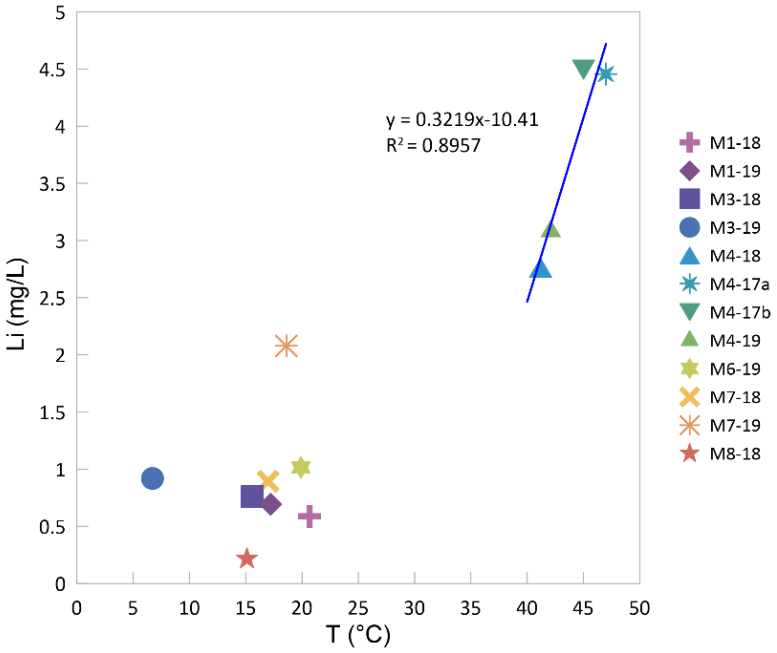

Figure 5: Lithium content versus water temperature

4.1.2 Lithium concentration and pH

Figure 6 shows Li concentrations versus pH. Although the samples with higher Li content (M4 in this case) are generally more acidic, as described by various workers (Munk et al., 2000; Zampirro 2004; Price, 2000; Hickson and Coolbaugh, 2017), the observed trend shows a poor correlation with R^2=0.34.

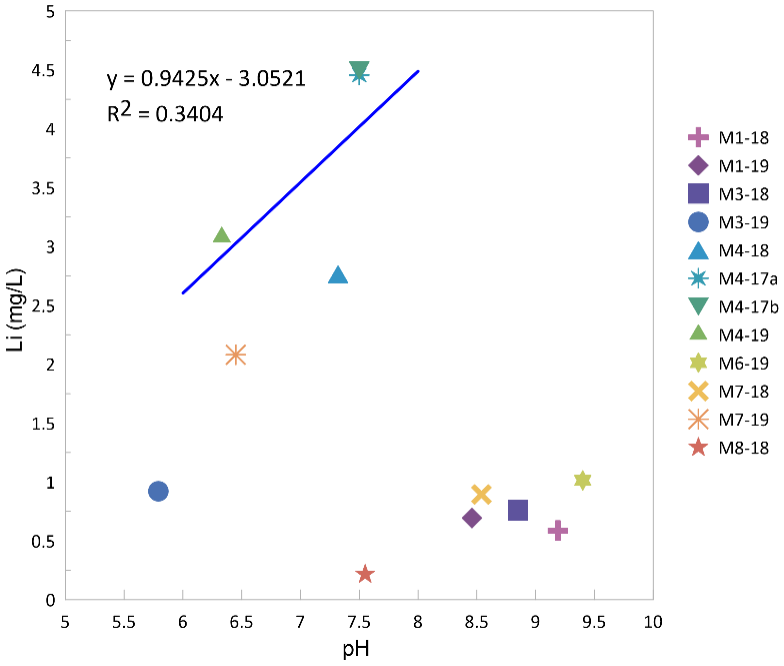

Figure 7: Lithium versus pH

4.1.3 Li and fluoride concentrations

On the other hand, Figure 8 shows relative concentrations of Li versus fluorine (F) that show a good correlation with R^2=0.84. Fluorine is an indicator of volcanic components in geothermal fluids that indicate the origin of these fluids. Additionally or alternatively, the constant Li/F ratio suggests the same source of both these elements, namely the volcanic rocks forming the reservoir for geothermal fluids.

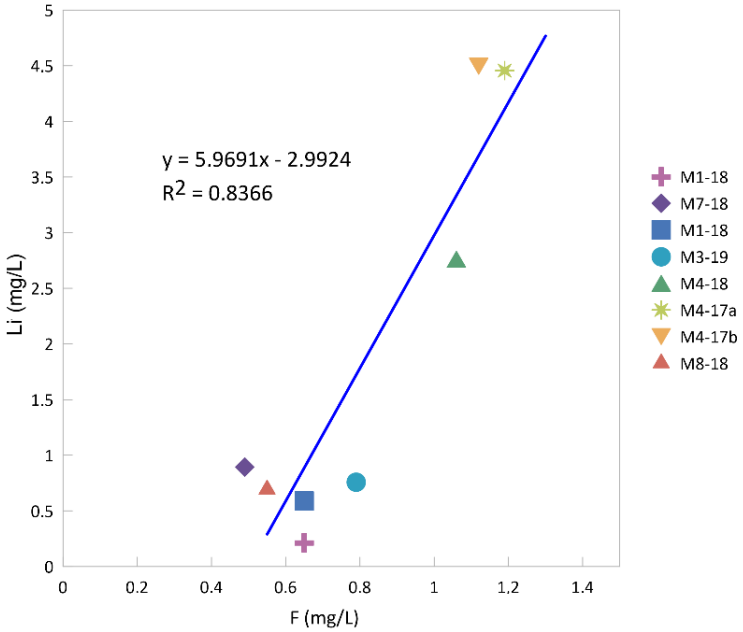

Figure 8: Li versus fluorine contents

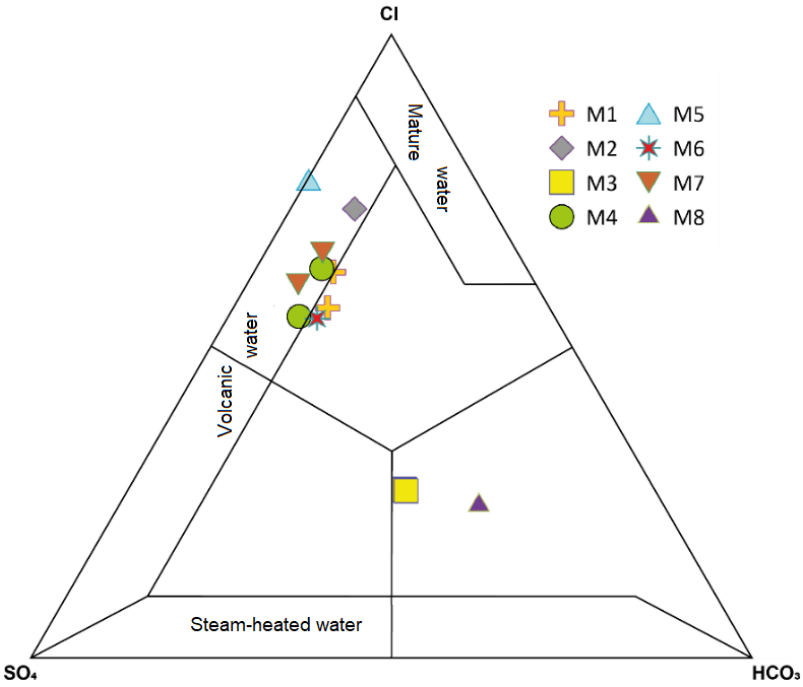

Figure 9: Relative Cl, SO_4 and HCO_3 contents (Giggenbach, 1991). Note: M3 and M8 are river waters.

4.1.4 Relative Cl, SO_4 and HCO_3 contents

Figure 9 presents normalized values of Cl, SO_4, and HCO_3 (Giggenbach, 1991) to identify the origin of thermal springs. The chloride could have its origin from geothermal fluids and the accumulation of residual salts as an effect of evapoconcentration. On the other hand, M3 and M8 have fewer chloride components, probably due to mixing of meteoric water (Nicolson, 1993).

4.1.4 Relative Li, Rb, and Cs contents

The ternary diagram of rare alkaline metals (Li, Rb. Cs; Figure 10) indicates that the waters evolve from the trend of rhyolitic rocks. All the thermal samples with a high Li/Cs indicate an outflow zone, is differentiated. The high Li/Cs suggests incorporation of Cs in zeolites, while low Li/Cs, as in the case of M8 site samples (outside the SLV basin) indicate incorporation of Li in quartz.

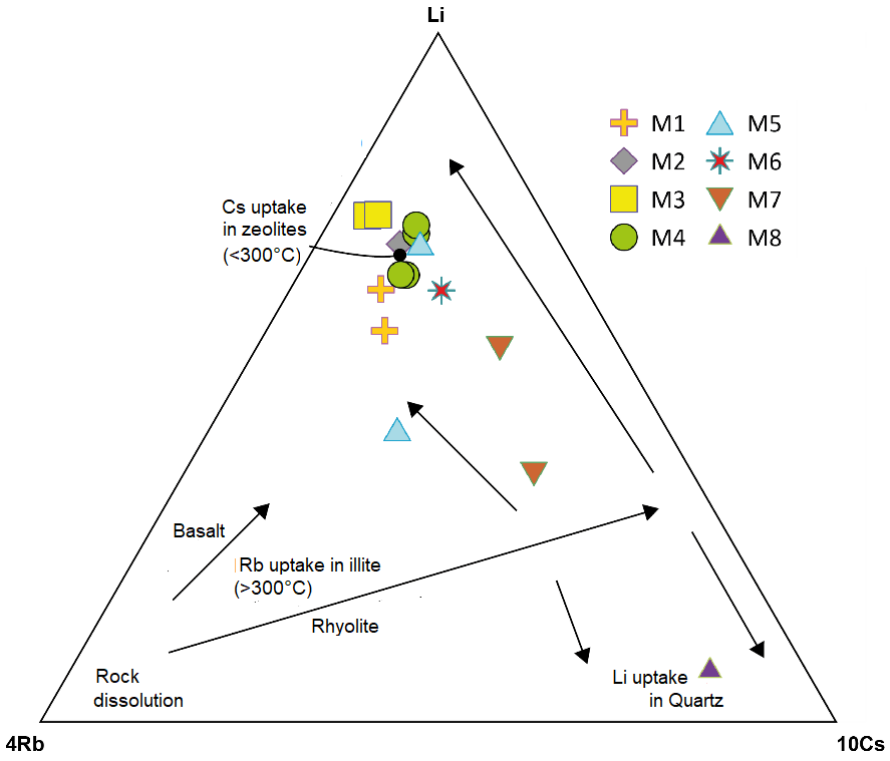

Figure 10: Relative Li, Rb and Cs contents (Giggenbach, 1991)

4.1.5 Relative Cl, B and Li contents

The ternary diagram Cl, B, and Li (Figure 11) is used since the B/Cl ratio indicates thermodynamic conditions, as B is volatile and increases the acidity of the water (with a relative increase of the HCl component). Li is used as a tracer for the initial process of rock dissolution and to evaluate the origin of Cl and B. Thermal water samples of site M4 are located in the low B/Cl region, indicating boron loss in the volatile phase, which suggests low temperatures or long duration. The variation in the B/Cl ratio for the M4 samples could be due to the dilution by meteoric waters derived from snowmelt.

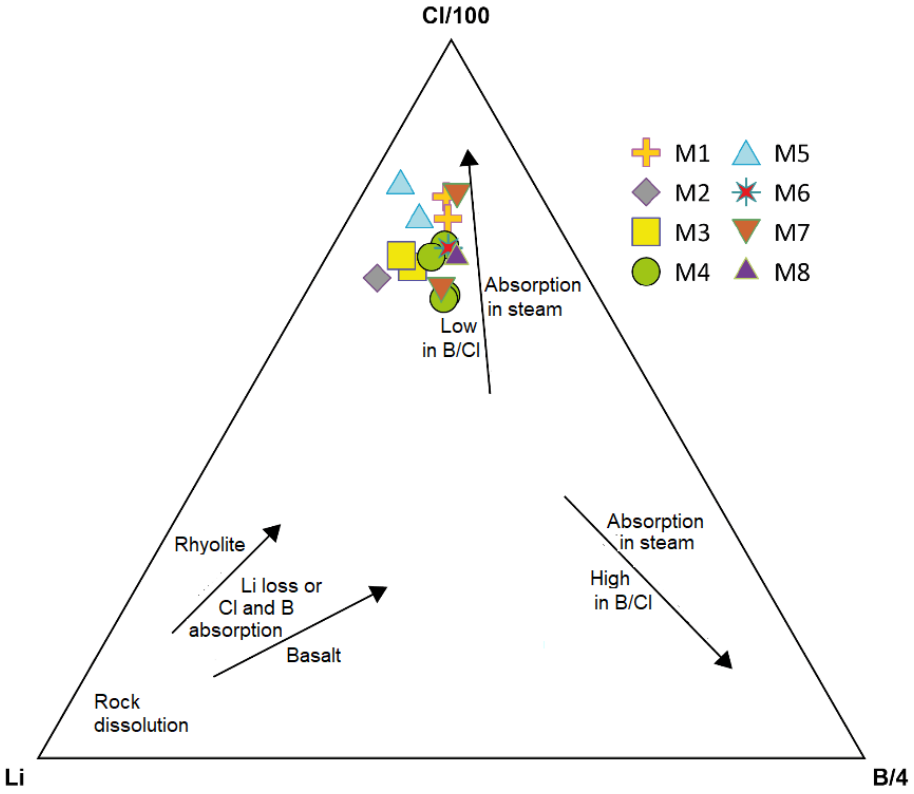

Figure 11: Relative Cl, B and Li contents (Giggenbach, 1991)

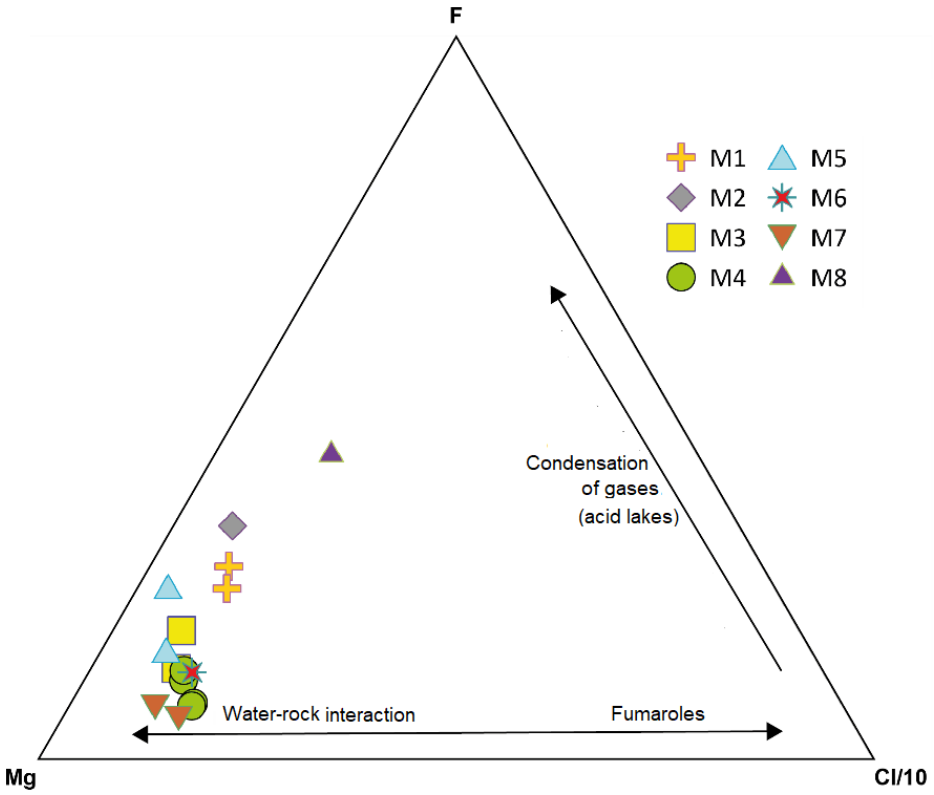

Figure 12: Ternary diagram F, Cl, and Mg

4.1.6 Relative F, Mg, and Cl contents

The relative contents of F, Mg, and Cl allow evaluating whether the fluids derive from the condensation processes of geothermal vapors or the rock-water interaction. Fluoride is a volcanic component, more abundant in upflow zones, while the interaction favors the release of Mg from rocks with higher temperature waters. In Figure 12, it can be seen that most of the water samples are located in the region where the water-rock interaction predominate.

4.2 Geothermometry

Figure 13 shows Na-K-Mg cationic geothermometer (Giggenbach, 1988), which estimates reservoir temperatures up to 85°C for the samples within partial equilibrium (M4-17a and M4-17B). Geothermal fluid samples outside this range (M4-18 and M4-19) in immature water field may be due to mixing processes with meteoric waters, as these were sampled after snow melting.

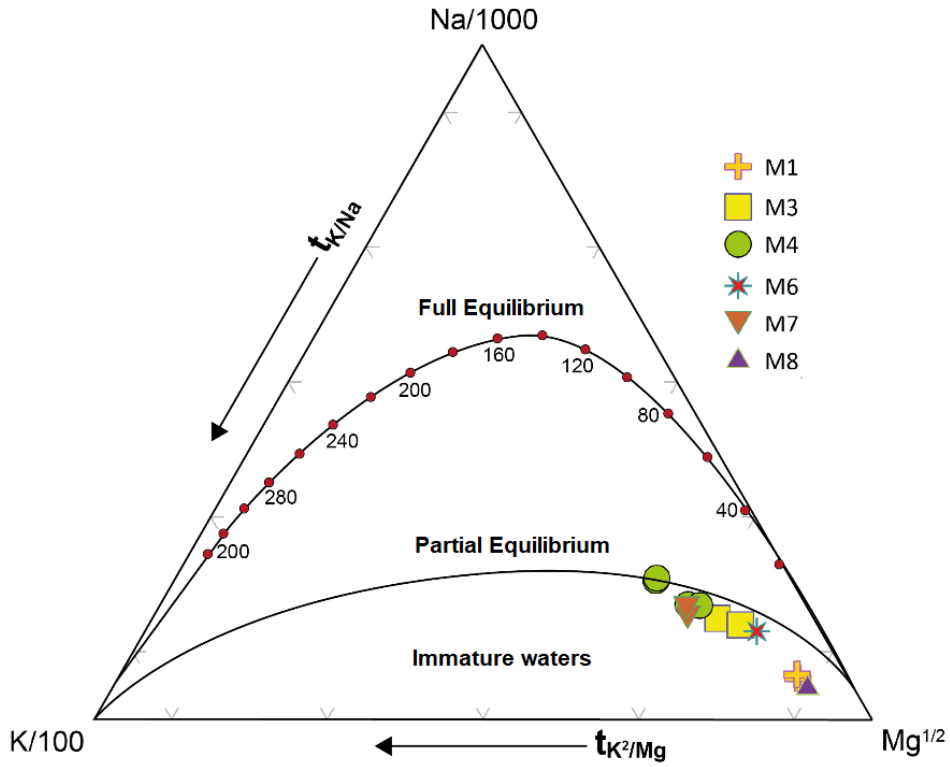

Figure 13: Na-K-Mg geothermometer (Giggenbach, 1988)

On the other hand, silica geothermometers (Fournier, 1977) indicate reservoir temperature of ~ 90 to 93°C and ~ 92 to 95°C, without and with maximum steam loss at 100°C, respectively. On the other hand, the quartz geothermometers proposed by Arnórsson (1998), which has a larger empirical database, give temperature ranges of ~76 to 79°C and 72°C without and with maximum vapor loss at 100°C, respectively. On the other hand, chalcedony geothermometers indicate lower temperatures in the range of ~59 to 64°C. Thus, although the estimated temperatures of the reservoir are below boiling point (100°C) under normal conditions, the theoretical boiling point at 6,400 m a.m.s.l. is 75.68°C. Different authors mention that the application of SiO_2 geothermometers has presented problems in the estimation of temperature due to chemical re-equilibrium, fluid mixing, and steam losses, as well as issues related to their

analytical determination (Nicholson, 1993). However, the cationic geothermometers do not present these difficulties because they are based on ionic relationships and not on the concentration of a chemical species (Fournier, 1977; Fournier and Potter, 1982; Arnórsson and Svavarsson, 1985; Rodriguez et al., 2008). Consequently, the temperatures obtained from the cationic geothermometers are considered more reliable than silica geothermometers.

Although the estimated temperatures of the reservoir are below boiling point under normal conditions, the considerable distance between the outflow and upflow zones (>25km) may indicate change(s) in chemical equilibrium that underestimate the reservoir temperature. In addition, the presence of the fumarole in the crater of the Nevado Ojos del Salado volcano suggests a system with vapor and liquid phases, which contradict the low temperatures estimated using different geothermometers. Further, there are likely permeability zones (faults) that infiltrate meteoric waters to geothermal flows in their path to the outflow zone, producing changes in the chemical balance and underestimating temperatures.

4.3 Isotopic composition

Figure 14 shows the isotopic variation (δD versus $\delta^{18}O$) reported with respect to SMOW (Standard Mean Ocean Water) with three lines representing the Global Meteoric Water Line (GMWL; Craig, 1962), the Local Meteoric Water Line (LMWL; Troncoso, 2012) and the Local Evaporation Line (LEL; Boschetti et al., 2019). The waters are enriched in $\delta^{18}O$, which can be explained by (i) isotopic enrichment of $\delta^{18}O$ due to the dissolution of rocks, where these isotopes are more abundant relative to ^{2}H o D, and/or ii) evaporation that concentrates heavier isotopes because of their weight, in the liquid phase. It is probably due to both the mechanisms for the thermal discharges at the SLV.

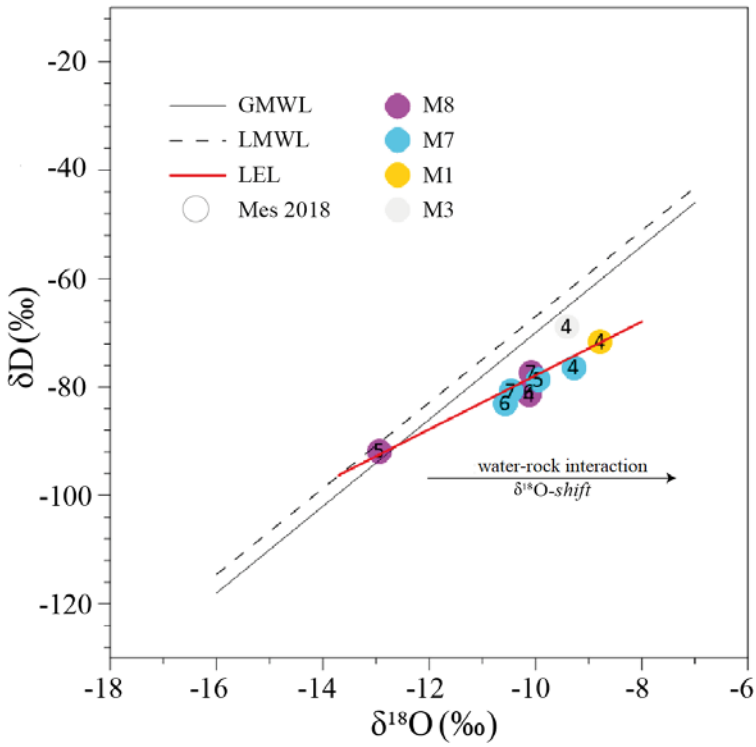

Figure 14: Isotopic variation δD and δ18O for different waters in the SLV

4.4 Geothermal system

The geothermal system that gives rise to the chloride waters emerging on the southern edge of Laguna Verde is potentially associated with the fumaroles of the central crater of the Nevado Ojos del Salado volcano. The low equilibrium temperatures from (85 to 95°C) derived from geothermometers are probably due to the considerable distance (>25 km) between the upflow and outflow zones. The changes in chemical equilibrium thus underestimate the geothermal reservoir temperature. However, it is also recommended to look for the heat sources (and upflow zone) in the El Muerto volcano of similar age to the Nevado Ojos del Salado. The former is closer to Laguna Verde but little explored. Based on the current understanding, i.e. outflow in Laguna Verde and upflow in Nevado Ojos del Salado, the authors propose Laguna Verde geothermal system (Figure 15) as a high-relief dynamic geothermal system with andesitic magmas as the heat source.

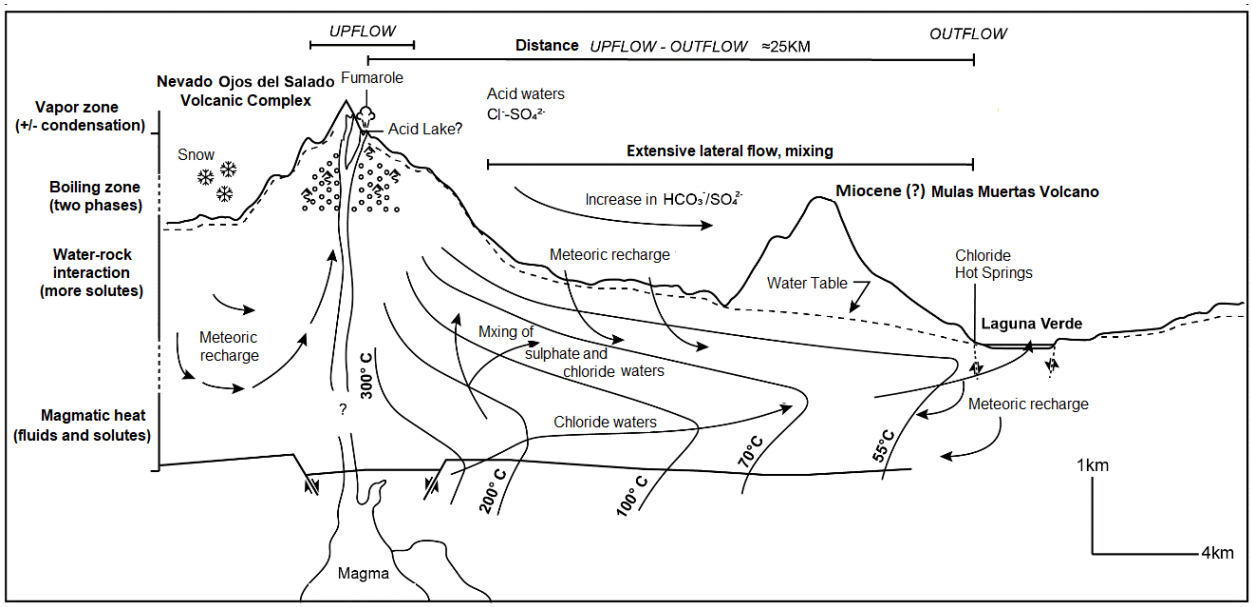

Figure 15: Schematic profile of the Nevado Ojos del Salado -Laguna Verde geothermal system

4.5 Li enrichment in the SLV

The rocks that constitute the filling and basement of the Laguna Verde basin that also serve as a source of Li are of andesitic and dacitic compositions for the most part. However, there are also rhyolitic rocks in more minor and basaltic in negligible quantity for the scale of this study. Although Li is more abundant in felsic rocks, especially those with higher vitreous content, the compositional distribution of rocks at the subsoil level, where most of the rock water interaction processes occur, is heterogeneous. Therefore, rocks of different compositions acted as Li sources by interacting with geothermal fluids associated with volcanic activity ongoing since the Late Miocene. With the data collected in this study, it is impossible to differentiate the formations based on their individual Li contribution. For this differentiation, it is necessary to perform a chemical analysis of the rocks of different compositions and subject these rocks to interaction with water of variable temperature and pH for different time intervals to measure the amount of Li released in each case. This will be done as part of another project.

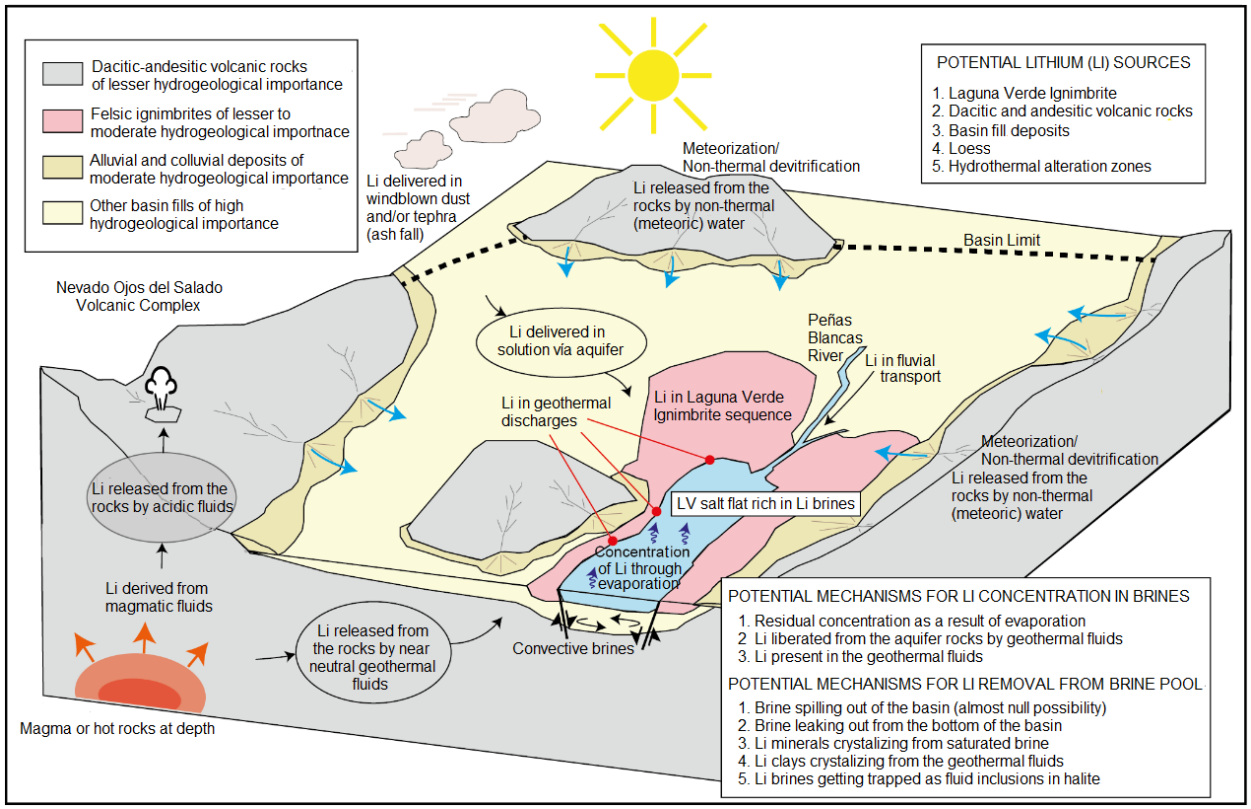

Figure 16: Diagram of the sources, pathways, and sinks of Li in the Salar de Laguna Verde, based on the Bradley (2013) Li brines enrichment model.

Considering the above, figure 16 shows a simplified scheme with the sources, flow paths, and sinks of Li to explain the geochemical processes responsible for the chemical composition of the waters in the SLV. Within the basin, the rocks of the rhyolitic composition of the Laguna Verde Ignimbrite and those rich in glass are considered more critical for their relatively high Li content. In contrast, the andesitic and dacitic rocks are deemed essential for their greater extension (lavas and volcanic complexes). Li is also released from basin-fill deposits, wind-transported sediments, and hydrothermal alteration zones to circulating meteoric waters. These sources release Li into the flows by non-thermal devitrification at shallow depth and by geothermal fluids at depth, the latter being more important, with up to 7 times more concentrated in Li.

5. Conclusions

The Li concentrations of the hot springs of Laguna Verde range from 4.49 to 2.76 mg/L, decreasing as a result of snow melting in the summer. Meanwhile, the recharges from the Falso Azufre Volcano and Agua Dulce River, which (based on the geologic evidence collected in this study, do not have geothermal inputs) have Li concentrations of 0.59 and 0.76 mg/L, respectively. This highlights the role of geothermal fluids in forming Li-enriched brines, which increases by at least an order of magnitude or up to 7.6 times the enrichment processes in a volcanic environment, such as the SLV. Mixing between thermal and non-thermal waters is evident in the samples M7-19 (Peñas Blancas River) and M6-19 (a tributary of the Peñas Blancas River) with concentrations of 2.08 and 1.01 mg/L, respectively. It also suggests the direction of geothermal flow from the Nevado Ojos del Salado volcano towards Laguna Verde.

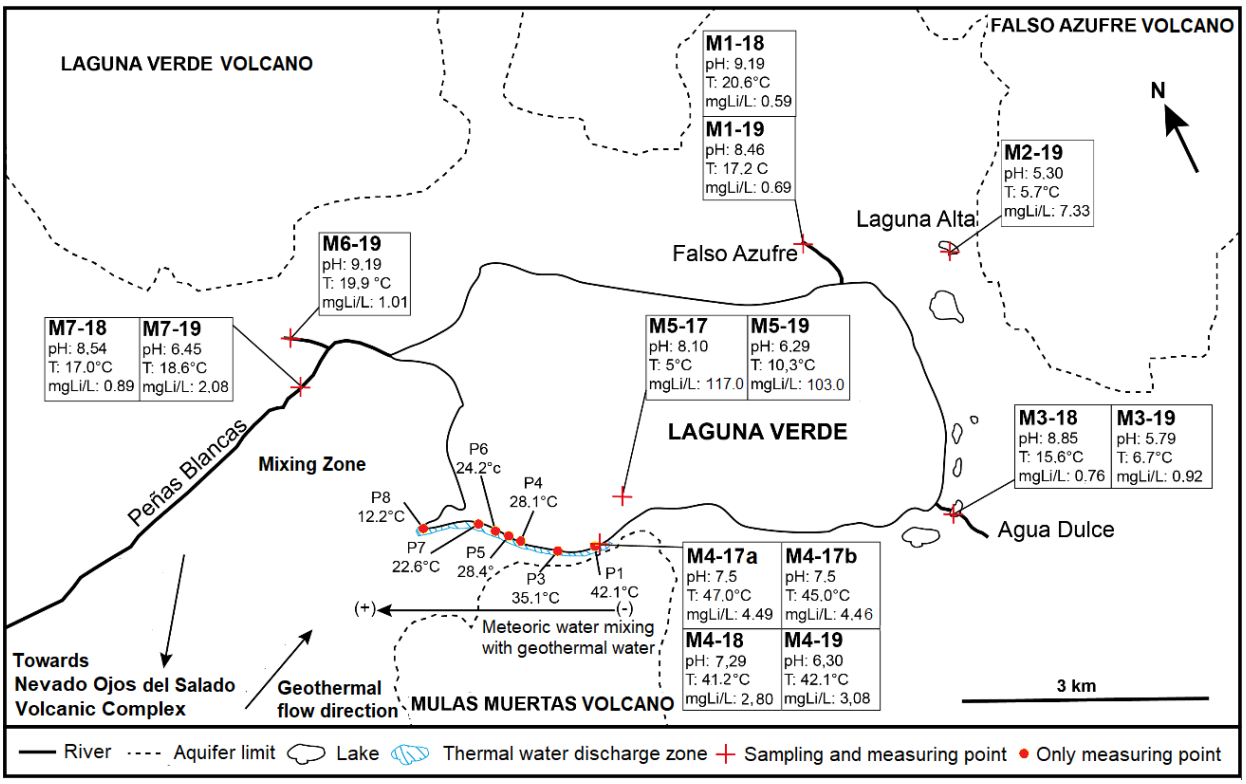

Figure 17: Diagram of the temperatures, pH, and Li concentrations measured in the different water bodies of the SLV. Note that samples M7 and M6 indicate that there is mixing with thermal waters from the SSW.

The Li concentrations in the streams without apparent geothermal fluids input, namely M1 and M3 with 0.59 and 0.76 mg/L, are at least four orders of magnitude higher than typical Li concentrations in the freshwater of less than 0.001 to 0.003 (Oram, 2014). This indicates that other processes of enrichment of Li involve only meteoric waters in addition to geothermal fluids. These processes could be due to (i) the high evaporation rates of the place that precipitates Li salts in the surface and groundwater, (ii) the intense alteration produced by volcanism from the Miocene to the Present that facilitates Li release from its source rocks, (iii) the abundance of volcanic rocks rich in glasses that release Li by non-thermal devitrification processes, and (iv) mixing with deep geothermal waters.

Acknowledgement

Some of the isotope data were facilitated by Project 16IFI-65907 of the Universidad de Atacama, which are indicated by asterisks (*) in the isotopic data presented here. Field visits and sample analysis were also supported by FIC-R Atacama Project Trampa de Nieves (Snow trap designs to enhance water resources in the Atacama Region; BIP 40013513). In addition, a field trip to the study area was carried out as a part of the VIII ENEGEOL (National Convention of Geology Students), during which three samples were collected.

REFERENCES

Arnórsson, S. "Interpretation of Chemical and Isotopic Data on Fluids Discharged from Wells in the Momotombo Geothermal Field with Notes on Gas Chromatography Analysis." *Project NIC/8/008-05*, Report on an expert mission to Nicaragua May 30th to June 13th 1998, Science Institute, University of Iceland, Reykjavík, Iceland (1998).

Arnórsson, S., and Svavarsson, H. "Application of Chemical Geothermometry to Geothermal Exploration and Development." *GRC Transactions*, 9, (1985), 293-298.

Baker, P.E., González-Ferrán, O., and Rex, D.C. "Geology and Geochemistry of the Ojos del Salado Volcanic Region, Chile." *Journal of the Geological Society*, 144(1), (1987), 85-96.

Boschetti, T, Cifuentes, J., Lacumin, P., and Selmo, E. "Local meteóric water line of Northern Chile (18 S–30 S): An application of error-in-variables regression to the oxygen and hydrogen stable isotope ratio of precipitation." *Water*, 11(4), (2019), 791.

Bradley, D., Munk, L., Jochens, H., Hynek, S., and Labay, K. "A Preliminary Deposit Model for Lithium Brines." *U.S. Geological Survey Open-File Report 2013–1006*, US Department of the Interior, US Geological Survey, Reston, Virginia (2013).

Camus, M. "Volcán Ojos del Salado – 6893 m. Andes Handbook,." Sociedad Geográfica de Documentación Andina, Santiago, Chile, (2001) Published 11/01/2001. Updated 12/14/2017. Available at: https://www.andeshandbook.org/montanismo/cerro/8/Ojos_del_Salado

Charrier, R., Pinto, L., and Rodríguez, M.P. (2007). "Tectonostratigraphic Evolution of the Andean Orogen in Chile." In: Moreno, T., and Gibbons, W. (Eds.), *The Geology of Chile*, 21-114.

Clavero, J., Mpodozis, C., and Gardeweg, M. "Mapa geológico del área del Salar de Wheelwright, Región de Atacama." Servicio Nacional de Geología y Minería, Mapas Geológicos (versión preliminar), Santiago, Chile (1997).

Clavero, J., Mpodozis, C., Gardeweg, M., and Valenzuela, M. "Geología de las Áreas Laguna Wheelwright y Paso San Francisco, Región de Atacama, Escala 1:100.000. Carta Geológica de Chile, Serie Geología Básica, n° 139-140." Servicio Nacional de Geología y Minería (SERNAGEOMIN), Santiago, Chile (2012).

Craig, H. "The Isotopic Geochemistry of Water and Carbon in Geothermal Areas." In: *Nuclear Geology in Geothermal Areas*, Consiglio Nazionale delle Ricerche, Laboratorio di Geologia Nucleare, Pisa, Italy (1963), 17-53.

Davis, J.R., Friedman, Irving, and Gleason, J.D. "Origin of the Lithium-rich brine, Clayton Valley, Nevada." *U.S. Geological Survey Bulletin*, 1622, (1986), 131-138.

EDRA (1999). "Hidrogeología sector quebrada Piedra Pómez." Compañía Minera Casales (unpublished).

Fouillac, C., and Michard, G. "Sodium/Lithium Ratio in Water Applied to Geothermometry of Geothermal Reservoirs." *Geothermics*, 10(1), (1981), 55-70.

Fournier, R.O., and Potter, R.W. II. "An Equation Correlating the Solubility of Quartz in Water from 25°C to 900°C at Pressures up to 10,000 bars." *Geochimica Cosmochimica Acta*, 46, (1982), 1969-1974.

FOURNIER, R.O. "Chemical Geothermometers and Mixing Models for Geothermal Systems." *Geothermics*, 5, (1977), 41-50.

Giggenbach, W.F. Geothermal Solute Equilibria. "Derivation of Na-K-Mg-Ca Geoindicators." *Geochimica Cosmochimica Acta*, 52, (1988), 2749-2765

Giggenbach, W.F. "Chemical Techniques in Geothermal Exploration." In: D'Amore, F. (Ed.), *Application of Geochemistry in Geothermal Reservoir Development*. UNITAR/UNDP Center on Small Energy Resources, Roma, Italia, (1991), 119-144.

González, G., Cembrano, J., Aron, F., Veloso, E.E., and Shyu, J.B.H.. Coeval Compressional Deformation and Volcanism in the Central Andes, Case Studies from Northern Chile (23 S–24 S). *Tectonics*, 28(6), (2009), TC6003.

Hickson, C., and Coolbaugh, M. "Do Geothermal Systems Play a Role in Lithium Brine Enrichment in Nevada Playas?" *GRC Transactions*, 41, (2017), 1922-1937.

Hiner, J.E. "Laguna Verde Salar Project and other Salar Properties held by South American Lithium Company S.A." *43-101 Technical Report*, Etna Resources Inc., Copiapó, Chile (2009)

Houston, J., Butcher, A., Ehren, P., Evans, K., and Godfrey, L. "The evaluation of brine prospects and the requirement for modifications to filing standards." *Economic Geology*, 106, (2011), 1225-1239.

Kesler, S.E., Gruber, P.W., Medina, P.A., Keoleian, G.A., Everson, M.P., and Wallington, T.J. "Global Lithium Resources: Relative Importance of Pegmatite, Brine and Other Deposits." *Ore Geology Reviews*, 48, (2012), 55-69.

Kharaka, Y.K., and Mariner, R.H. "Chemical geothermometers and their application to formation waters from sedimentary basins." In: Naeser, N.D. and McCulloh, T.H. (Eds.), Thermal History of Sedimentary Basins, Methods and Case Histories: Springer-Verlag, New York, NY (1989.

Lowenstein, T.K., and Risacher, F. "Closed Basin Brine Evolution and the Influence of Ca-Cl Inflow Waters: Death Valley and Bristol Dry Lake California, Qaidam Basin, China, and Salar de Atacama, Chile." *Aquatic Geochemistry*, 15, (2009), 71-94.

Munk, L., Boutt, D., Hynek, S., and Moran, B. "Hydrogeochemical Fluxes and Processes Contributing to the Formation of Lithium-enriched Brines in a Hyper-arid Continental Basin." *Chemical Geology*, 493, (2018), 37-57.

MWH. "Línea Base Hidrogeología EIA." Compañía Minera Casale, Santiago, Chile (2011).

Nicholson, K. "Geothermal Fluids: Chemistry and Exploration Techniques." Springer-Verlag, Berlin (1993).

Oram, B. "Lithium in Groundwater, Drinking Water Marcellus Shale Water Testing." Water Research Center, Dallas, PA (2014).

Piper, A. "A Graphic Procedure in the Geochemical Interpretation of Water-Analyses." *Transactions American Geophysical Union*, 25(6), (1944), 914-928.

Price, J.G., Lechler, P.J., Lear, M.B., and Giles, T.F. "Possible Volcanic Source of Lithium in Brines in Clayton Valley, Nevada." In: Cluer, J.K., Price, J.G., Struhsacker, E.M., Hardyman,

R.F., and Morris, C.L. (Eds.), *Geology and Ore Deposits 2000: The Great Basin and Beyond, Proceedings Geological Society of Nevada Symposium*, Reno, Nevada (2000), 241-248.

Risacher, F., Alonso, H., and Salazar, C. "Geoquímica de Aguas en Cuencas Cerradas: I, II y III Regiones-Chile." *Convenio de Cooperación DGA – UCN – IRD* (1999).

Rodríguez, L., Santoyo, E., and Reyes, J. "Three New Improved Na/K Geothermometers Using Computational and Geochemiometrical Tools: Application to the Temperature Prediction of Geothermal Systems." *Revista Mexicana de Ciencias Geológicas*, 25(3), (2008), 465-482.

Santibáñez, I., Venegas, M., y Espinoza, C. "Hidrogeología de la cuenca Campo de Piedra Pómez - Laguna Verde, región de Atacama, Escala 1:100.000." *Carta Geológica de Chile, Serie Hidrogeología (n.4)*, Servicio de Minería y Geología (SERNAGEOMIN), Santiago, Chile (2006)

SKR. "Hidrogeología campo de Pozos Piedra Pómez, Rev. 4." *SEIA Compañía Minera Casale, Proyecto SKR 02-1087-18*, SKR Consulting, Santiago, Chile (2011).

Stern, C. Active Andean Volcanism: Its Geologic and Tectonic Settings. *Revista Geológica de Chile*, 37, (2004), 161-206.

Troncoso, R., Castro, R., Lorca, M.E., Espinoza, C., y Pérez, Y. "Análisis Preliminar de la Composición Isotópica Oxígeno 18 – Deuterio de las Aguas de la Cuenca del río Copiapó, Región de Atacama: Una Contribuciónal conocimiento del Sistema Hidrogeológico." *Proceedings of the XIII Congreso Geológico Chileno*, Antofagasta, Chile, (2012), 774-776.

Yu, J., Gao, C., Cheng, A., Liu, Y., Zhang, L. y He, X. "Geomorphic, Hydroclimatic and Hydrothermal Controls on the Formation of Lithium Brine Deposits in the Qaidam Basin, Northern Tibetan Plateau, China." *Ore Geology Reviews*, 50, (2013), 171-183.

Zampirro, D. "Hydrogeology of Clayton Valley Brine Deposits, Esmeralda County, Nevada." In: Castor, S.B., Papke, K.G., and Meeuwig, R.O. (Eds.), Betting on Industrial Minerals, Proceedings of the 39th Forum on the Geology of Industrial Minerals, Reno-Sparks, Nevada, *Nevada Bureau of Mines and Geology Special Publication 33* (2004), 271-280.